Supporting Information

ZIF-67/wood derived self-supported carbon composites for electromagnetic interference shielding, sound and heat insulations

Xiaofan Ma,[a] Zhichao Lou,[a*] Hongtao Guo,[a] Zhiwei Tian,[a] Donghe Chen,[c] Yifan Wang,[a] Yiming Chen,[a,d] Chunmei Zhang,[b*] Shiwei Wang,[c] Gaigai Duan,[a] Jingquan Han,[a] Changtong Mei,[a] Shaohua Jiang[a*]

[a] Jiangsu Co-Innovation Center of Efficient Processing and Utilization of Forest Resources, International Innovation Center for Forest Chemicals and Materials, College of Materials Science and Engineering, Nanjing Forestry University, Nanjing, 210037, China.

[b] Institute of Materials Science and Devices, School of Materials Science and Engineering, Suzhou University of Science and Technology, Suzhou 215009, China.

[c] School of Chemical Engineering, Changchun University of Technology, Changchun 130012, China.

[d] Key Laboratory of Urban Rail Transit Intelligent Operation and Maintenance Technology & Equipment of Zhejiang Province, College of Engineering, Zhejiang Normal University, Jinhua 321004, China.

Corresponding authors:

zc-lou2015@njfu.edu.cn (Z. Lou); shenbin@nimte.ac.cn (B. Shen); shaohua.jiang@njfu.edu.cn (S. Jiang)

Materials

Basswood was cut into cuboids measuring 50 mm × 40 mm × 5 mm. $Co(NO_3)_2·6H_2O$ (98%), 2-Methylimidazole (2-MeIm, $C_6H_6N_2$, 97%), and hexadecyl trimethyl ammonium bromide (CTAB, $C_{19}H_{42}BrN$, 99%) were purchased from Sigma-Aldrich. All aqueous solutions were prepared with deionized water.

Characterizations

The thermal stability of the samples was measured with a thermogravimetric analyzer (TG 209 F3, NETZSCH, Germany) under N_2 from 30 °C to 1000 °C at a heating rate of 10 °C min^{-1}. The specific surface area of the samples was determined by the Brunauer-Emmet-Teller (BET) method using the TriStar II 3020 system (Micromeritics, ASAP2460, USA). The structural and morphological information of the samples was obtained by field emission scanning electron microscopy (SEM) (Nova Nano 450, FEI, USA) and transmission electron microscopy (TEM) (JEOL, JEM-2100F, Japan). Raman spectra (Themor, DXR532, USA) were measured to analyze characteristics of carbon-related material. Magnetic hysteresis loops (LakeShore, 7404 magnetometer, USA) were recorded to provide hysteresis loops. X-ray powder diffraction (XRD) patterns were obtained using an X-ray diffractometer (DY-1291, Philips, Dutch) with a CuKα line. X-ray photoelectron spectra (XPS) (Thermo Scientific, ESCALAB 250Xi, USA) were recorded on an X-ray photoelectron spectrometer using Al Kα radiation. Acoustic analysis of the sample was measured by using Type SW-422 Impedance Tubes (BSWA Technology Co., Ltd, China) according to the transfer function method specified in ASTM E2611-17.

EMI calculations

The electrical conductivity of the carbon composites was calculated using a four-point probe method (Guangzhou Four-Point-Probe Technology, SDY-4, China). The relative complex permittivities and complex permeabilities of the samples were used in X-band using the coaxial line method (Agilent PNA N5224A vector network analyzer, USA). The samples were prepared by mixing 15% wt% samples and 85% wt% paraffin wax evenly and pressing it into toroidal-shaped (Fout: 7.0 mm, Fin: 3.04 mm). The EMI shielding effectiveness was measured with the Vector Network Analyzer (Agilent Technologies N5063A, USA). The test samples were carefully cut into 22.86 mm × 10.16 mm × 1.5 mm strips to fit the specific waveguide sample holders (8.2–12.4 GHz). EM waves can interact with EMI shielding materials via reflection, absorption, and transmission. According to the law of conservation of energy, the reflection coefficient (R), absorption coefficient (A) and transmission coefficient (T) can be expressed as:

$$R + A + T = 1 \qquad (1)$$

$$R = |S_{11}|^2 = |S_{22}|^2 \quad (2)$$

$$T = |S_{12}|^2 = |S_{21}|^2 \quad (3)$$

where S_{11} and S_{21} represent the reflection coefficient and the transmission coefficient, respectively. The total EMI shielding effectiveness (SE_T) can thus be divided into three aspects: the reflection effectiveness (SE_R) from the material surface, the absorption effectiveness (SE_A) originating from the magnetic and conduction losses, and the multiple reflection effectiveness (SE_{MR}) inside the materials. If SE_T exceeds 15 dB, SE_{MR} can be generally ignored. The shielding effectiveness of reflection and absorption can be rewritten using the following formulas:

$$SE_R = 10log\left(\frac{1}{1-R}\right) = 10log\left(\frac{1}{1-|S_{11}|^2}\right)$$

(4)

$$SE_A = 10log\left(\frac{1-R}{T}\right) = 10log\left(\frac{1-|S_{11}|^2}{|S_{21}|^2}\right)$$

(5)

$$SE_T = SE_R + SE_A \quad (6)$$

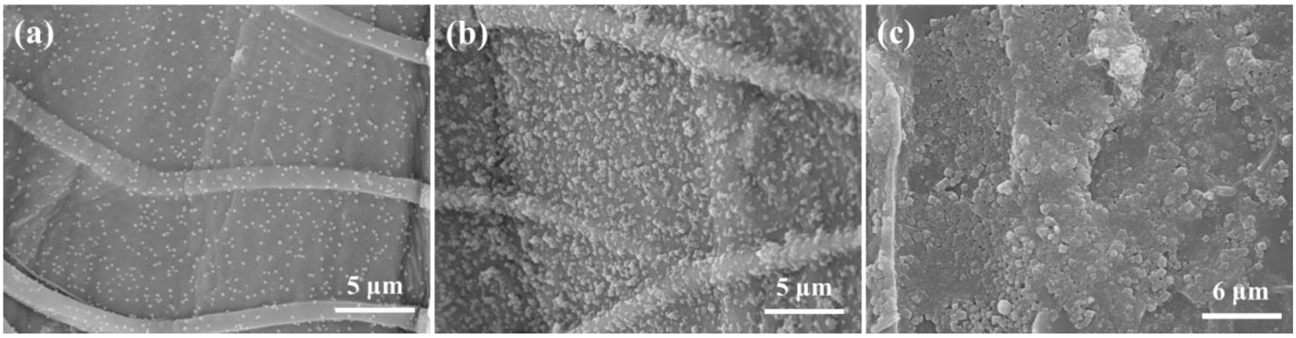

Figure S1. ZIF-67/wood samples with different content of ZIF-67 crystal.

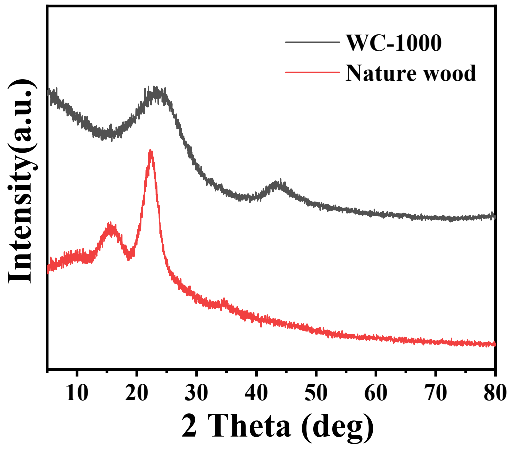

Figure S2. XRD pattern of nature wood and WC-1000

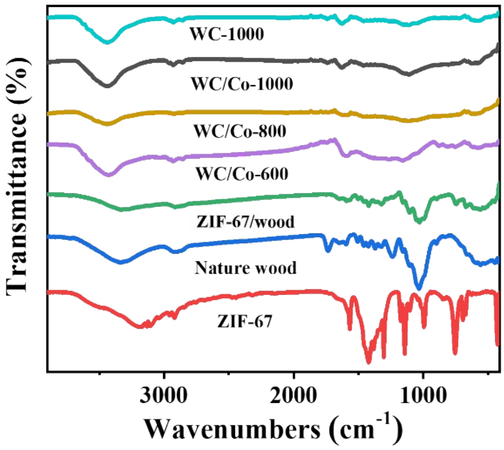

Figure S3. FTIR spectra of samples.

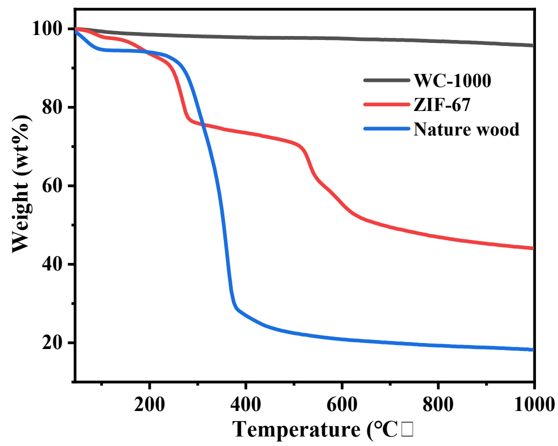

Figure S4. TG data of nature wood, ZIF-67 and WC.

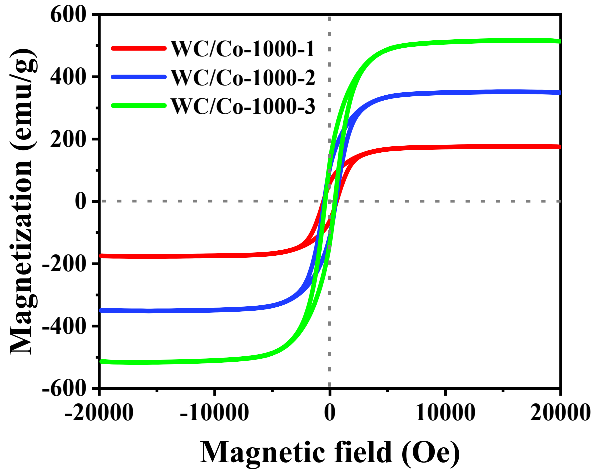

Figure S5. Magnetic hysteresis loops of WC/Co-1000-1, WC/Co-1000-2 and WC/Co-1000-3.

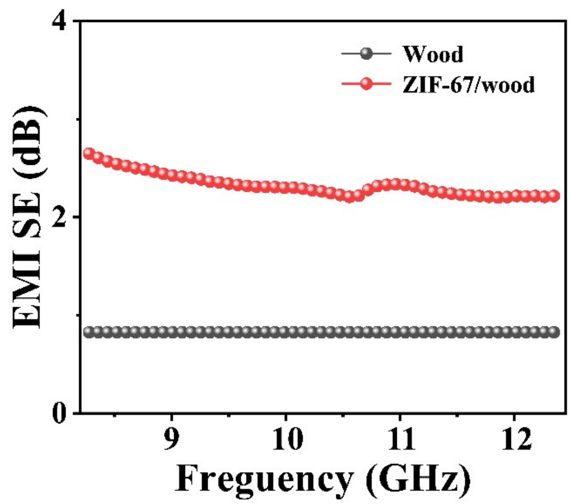

Figure S6. EMI-SE of wood, ZIF-67/wood.

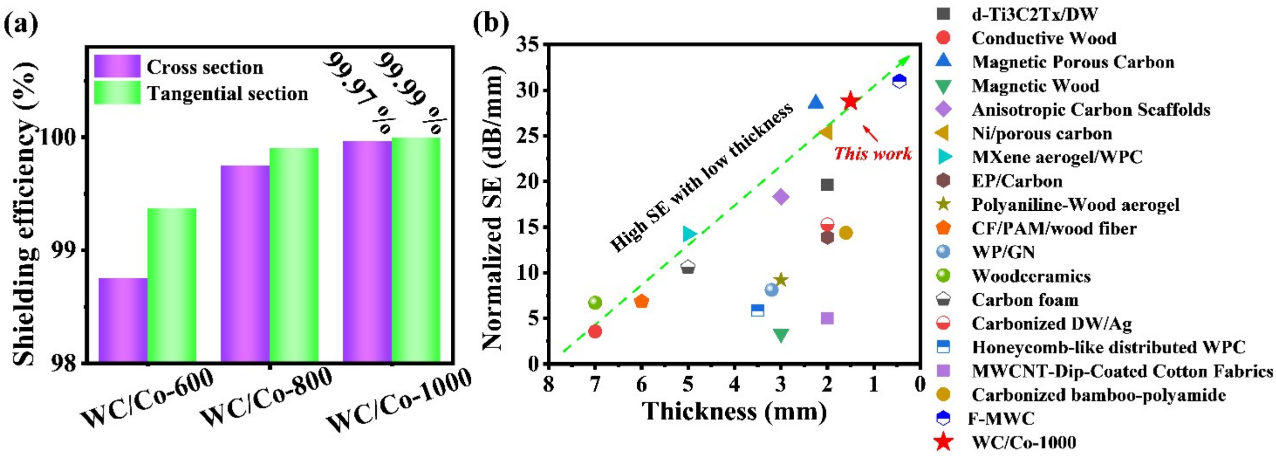

Figure S7. (a) EMI shielding efficiency of the Co/C@WC composites in the cross-section and the tangential section. (b) Values of normalized EMI SE_T/thickness for WC/Co-1000 and other reported wood-derived materials at 8.2–12.4 GHz.

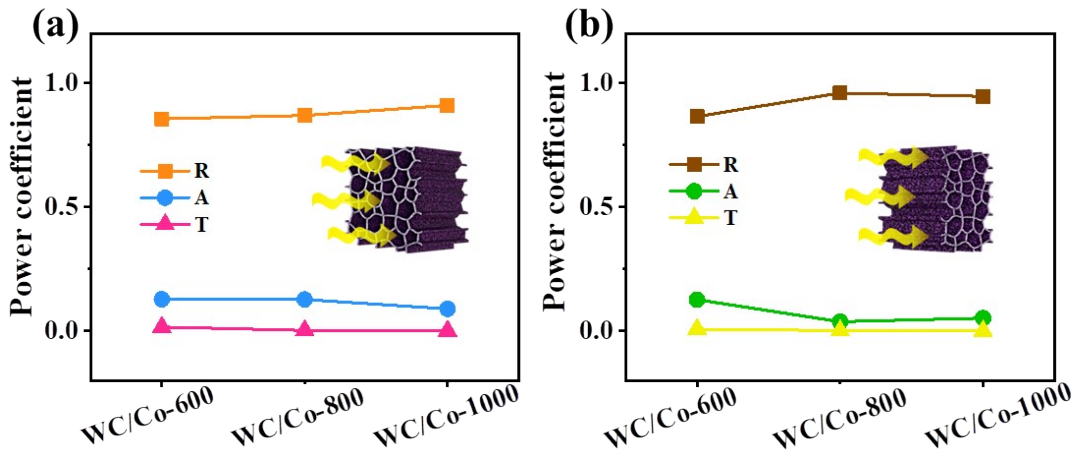

Figure S8. The corresponding average R, A and T values of Co/C@WC composites in cross section (a) and tangential section (b).

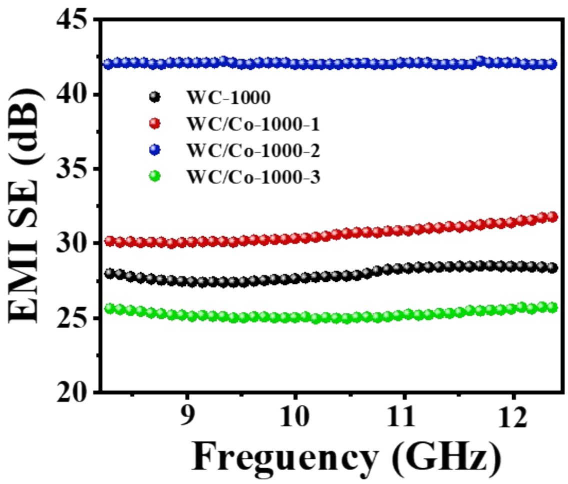

Figure S9. EMI-SE of WC-1000, WC/Co-1000-1, WC/Co-1000-2 and WC/Co-1000-3.

Table S1. WC/Co-1000 composites with different Co contents and their composition and electrical conductivity.

Samples	The content of Co (At. %)	The content of C (At. %)	The content of O (At. %)	The content of N (At. %)	The conductivity (S m^{-1})
WC/Co-1000-1	0.05	95.62	3.91	0.42	2586
WC/Co-1000-2	0.10	97.16	2.22	0.52	3247
WC/Co-1000-3	0.17	95.54	3.67	0.68	3069

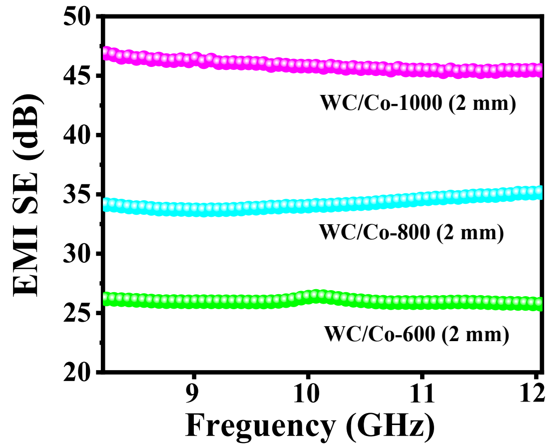

Figure S10. EMI-SE_T of Co/C@WC composites with 2 mm thickness in tangential section.

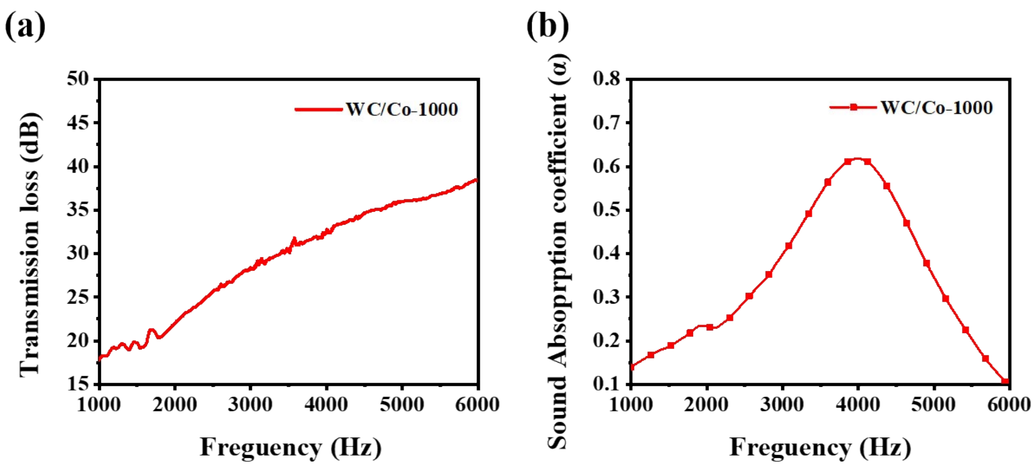

Figure S11. (a) Transmission loss and (b) sound absorption coefficient of WC/Co-1000.

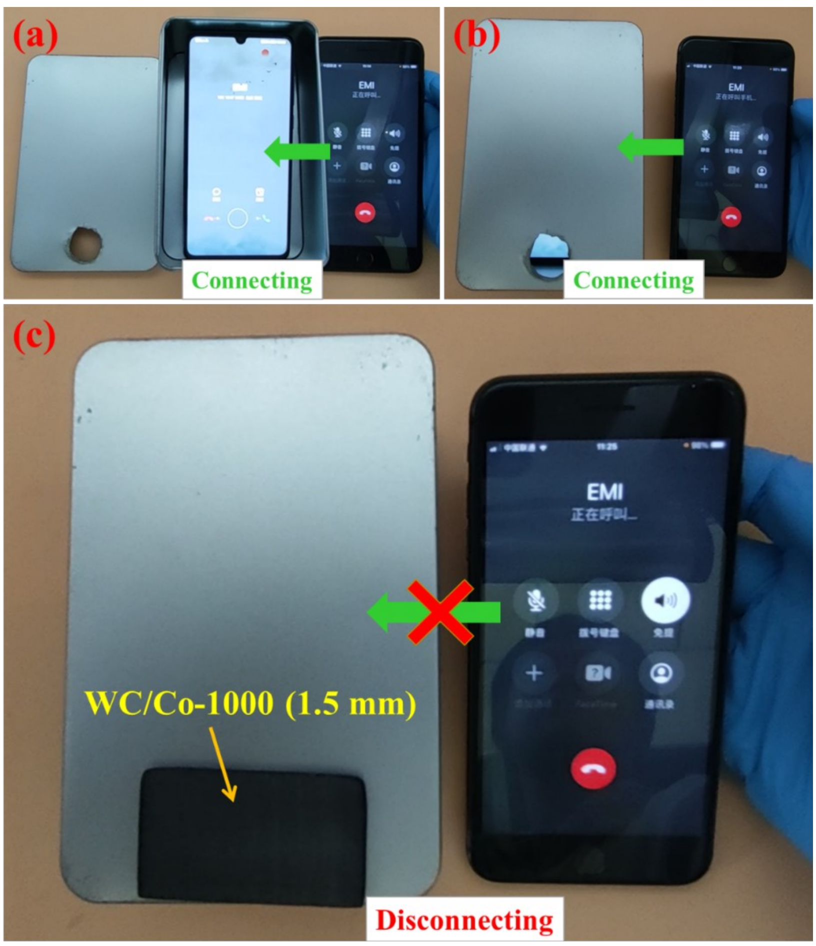

Figure S12. The realistic application simulation of the WC/Co-1000 (with a 1.5 mm thickness) for EMI shielding: (a) communication connecting with no EMI shielding materials, (b) communication connecting with an iron cover with a gap, and (c) communication disconnecting with an iron cover with a WC/Co-1000.

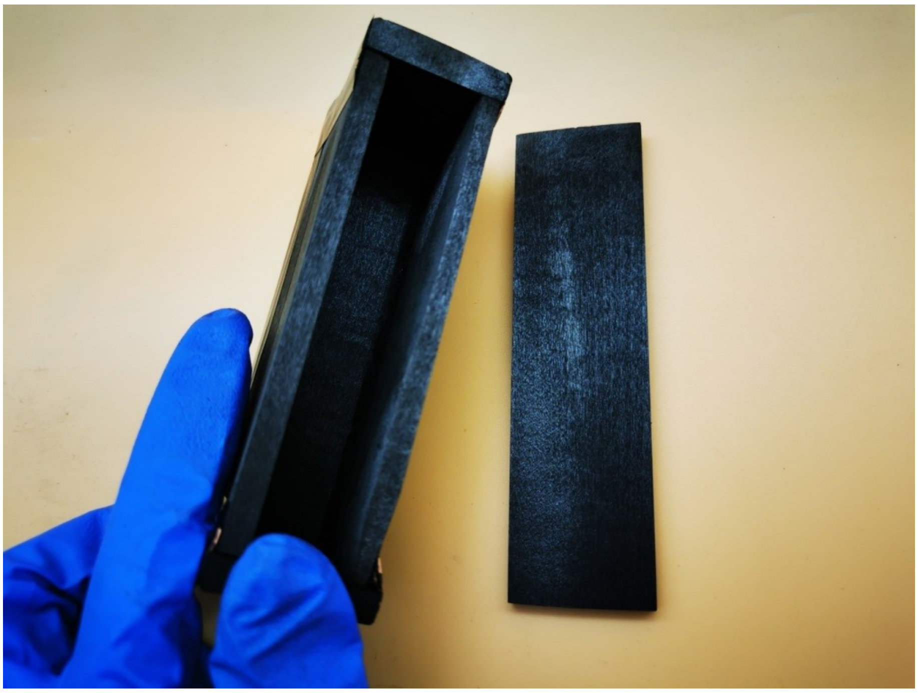

Figure S13. Photo of the box (EMI-M1000)

Figure S14. Electric field and magnetic field value of bluetooth signal before and after shielding.

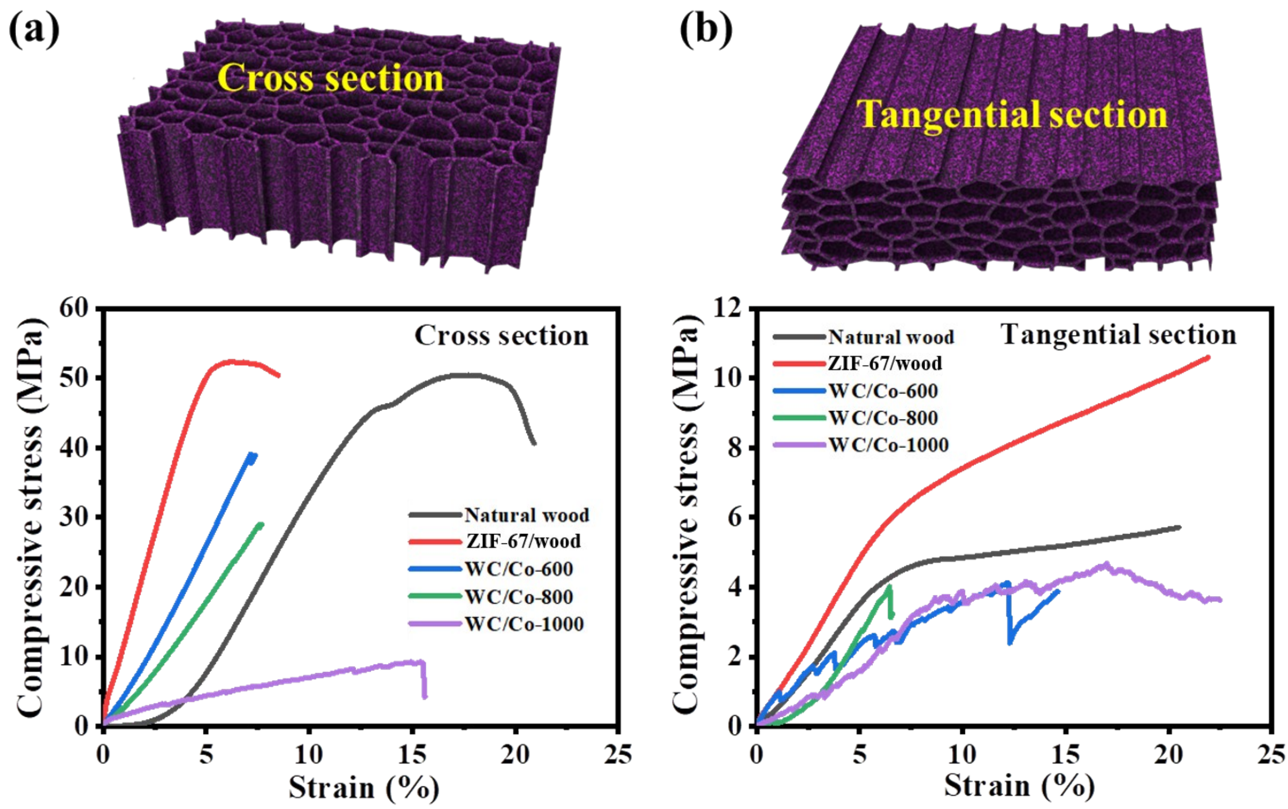

Figure S15. (a and b) Compressive stress-strain curves of the natural wood and ZIF-67/wood and Co/C@WC composites in cross section and tangential section.